Supporting Information

Hierarchical Nanostructures Created by Interference of High-Order Diffraction Beams

*Tae Yoon Jeon, Hwan Chul Jeon, Seung-Man Yang and Shin-Hyun Kim**

*E-mail address : kim.sh@kaist.ac.kr

S1. Fabrication procedure for conformable diffraction grating

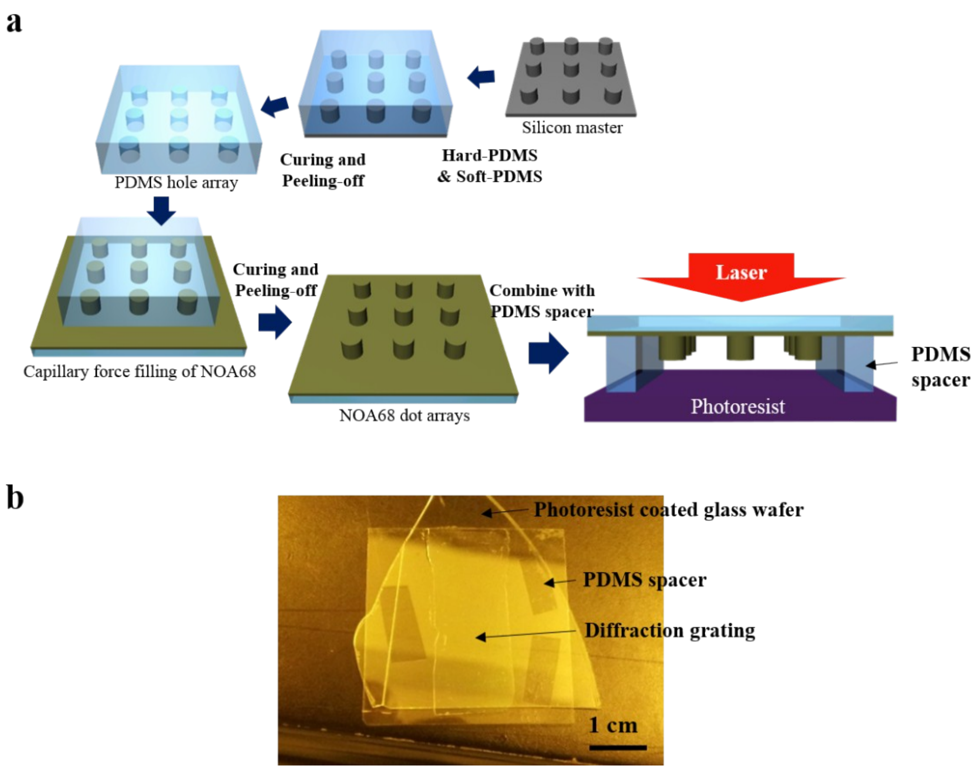

Figure S1. (a) Schematic diagrams showing the fabrication procedure for conformable phase mask. (b) A photo of diffraction grating mounted on photoresist-coated glass wafer with assistance of PDMS spacer.

S2. Relationship between PDMS thickness and spin speed

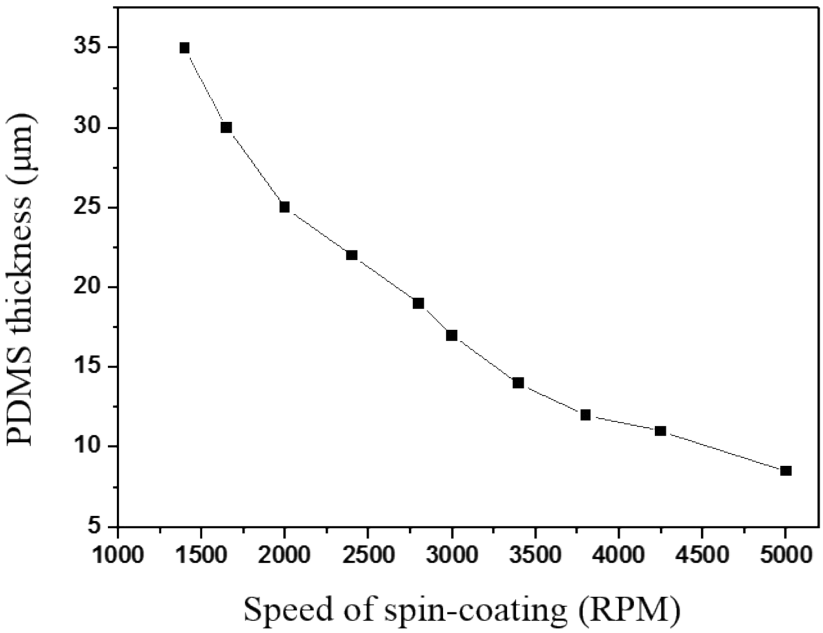

Figure S2. Thickness of PDMS spacer as a function of spinning rate.

S3. Calculation of Talbot distance and phase difference between 0th-and *m*th-order diffraction beams at *z*-planes

When *m*th-order diffraction beam propagates with diffraction angle, θ, optical path length between point O at the grating and point P in the beam path is given by

$$OP_m(y) = \frac{\lambda}{2\pi}\Phi \quad , \text{(S1)}$$

where Φ is phase difference between the two points and determined by

$$\Phi = \vec{k}\cdot\vec{r} = k_z z + k_y y = \frac{2\pi}{\lambda}\cos\theta S + \frac{2\pi}{\lambda}\sin\theta\, y \quad . \quad \text{(S2)}$$

Therefore, $OP_m(y)$ is expressed by following equation:

$$OP_m(y) = S\left(1 - sin^2\theta\right)^{\frac{1}{2}} + y\; sin\theta = S\left(1 - \frac{m^2\lambda^2}{d^2}\right)^{1/2} + y\frac{m\lambda}{d} \quad , \quad \text{(S3)}$$

where we use diffraction equation, $sin(\theta) = \frac{m\lambda}{d}$.

Therefore, optical path of *m*th-order diffraction beam on z-axis is

$$OP_m(0) = S\left(1 - \frac{m^2\lambda^2}{d^2}\right)^{1/2} \quad . \text{(S4)}$$

The optical path difference between 0th-order diffraction beam and 1st-order diffraction beam on the z-axis is therefore given by

$$OP_0(0) - OP_1(0) = S - S\left(1 - \frac{\lambda^2}{d^2}\right)^{1/2} = S\left[1 - \left(1 - \frac{\lambda^2}{d^2}\right)^{1/2}\right] . \quad \text{(S5)}$$

At every Talbot distance, 0th- and 1st-order diffraction beams should be in phase. Therefore, $OP_0(0)$ - $OP_1(0)$ should be $N\lambda$, at which $S = NZ_t$, where N is integer and Z_t is Talbot distance.

With this relation, the equation (S5) can be rearranged to provide equation for Z_t:

$$Z_t = \frac{\lambda}{1 - \left(1 - \frac{\lambda^2}{d^2}\right)^{\frac{1}{2}}} . \quad \text{(S6)}$$

From equation (S4), the optical path difference of 0th- and mth-order diffraction beams on a z-axis can be written as

$$[OP_0(0) - OP_m(0)]_z = z - z\left(1 - \frac{m^2\lambda^2}{d^2}\right)^{\frac{1}{2}} = z\left[1 - \left(1 - \frac{m^2\lambda^2}{d^2}\right)^{1/2}\right] . \quad \text{(S7)}$$

Therefore, the phase difference between 0th-and mth-order diffraction beams at z-planes, $\Delta\Phi_m(z)$ becomes

$$\Delta\Phi_m(z) = 2\pi z\left[1 - \left(1 - \frac{m^2\lambda^2}{d^2}\right)^{1/2}\right] . \quad \text{(S8)}$$

Arbitrary position, z, can be divided by Z_t to have equation for the phase difference on relative position:

$$\Delta\Phi_m(z) = 2\pi\lambda\frac{z}{Z_t}\left[\frac{1 - \left(1 - \frac{m^2\lambda^2}{d^2}\right)^{1/2}}{1 - \left(1 - \frac{\lambda^2}{d^2}\right)^{1/2}}\right] . \quad \text{(S9)}$$

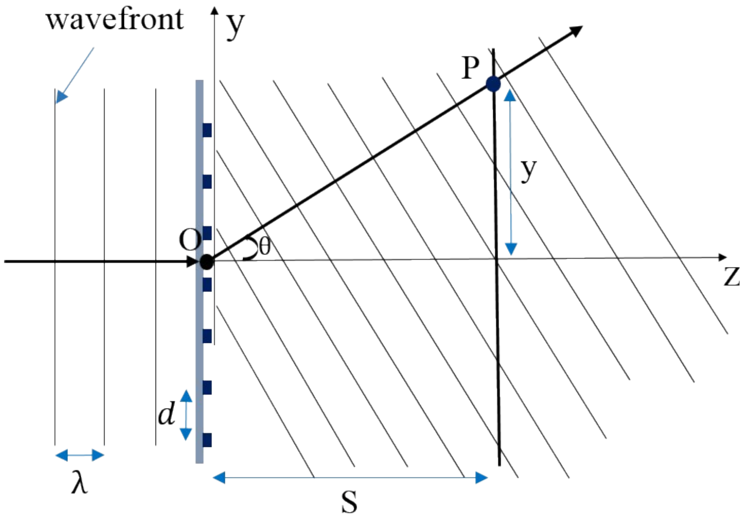

Figure S3. Schematic diagram of diffracted light when the incident light passing through diffraction grating. λ is wavelength of incident light, d is grating period and θ is the diffraction angle.

Reference : M. Daniel, *Optica Acta*, **1974**, 21, 631.

S4. 3D periodic nanostructure generated from 325 nm wave diffracted by 500 nm diffraction grating

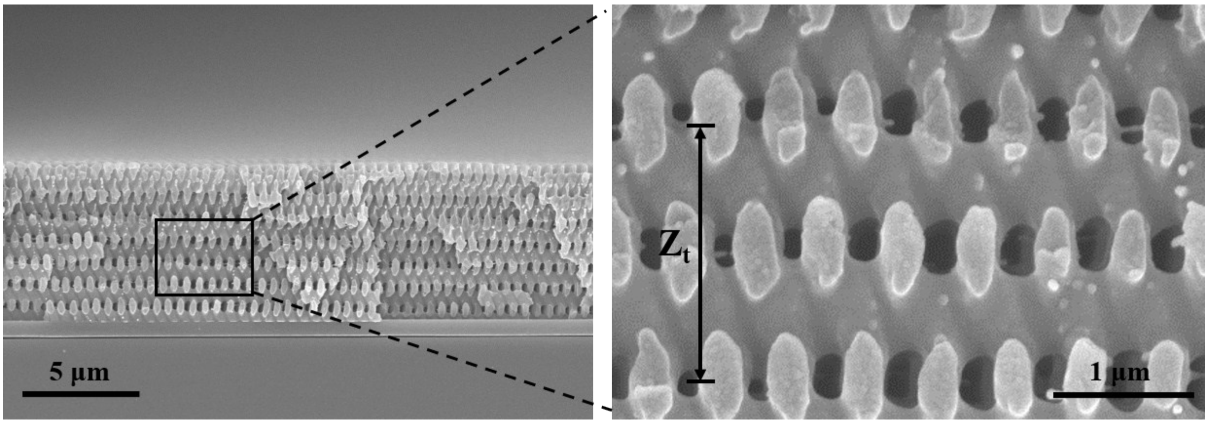

Figure S4. Cross-sectional SEM images of periodic 3D nanostructure prepared by transferring 3D periodic light intensity pattern into the negative photoresist.

S5. Horizontal sections of 3D light intensity profile formed by 500 nm grating with incident light with 325 nm wavelength.

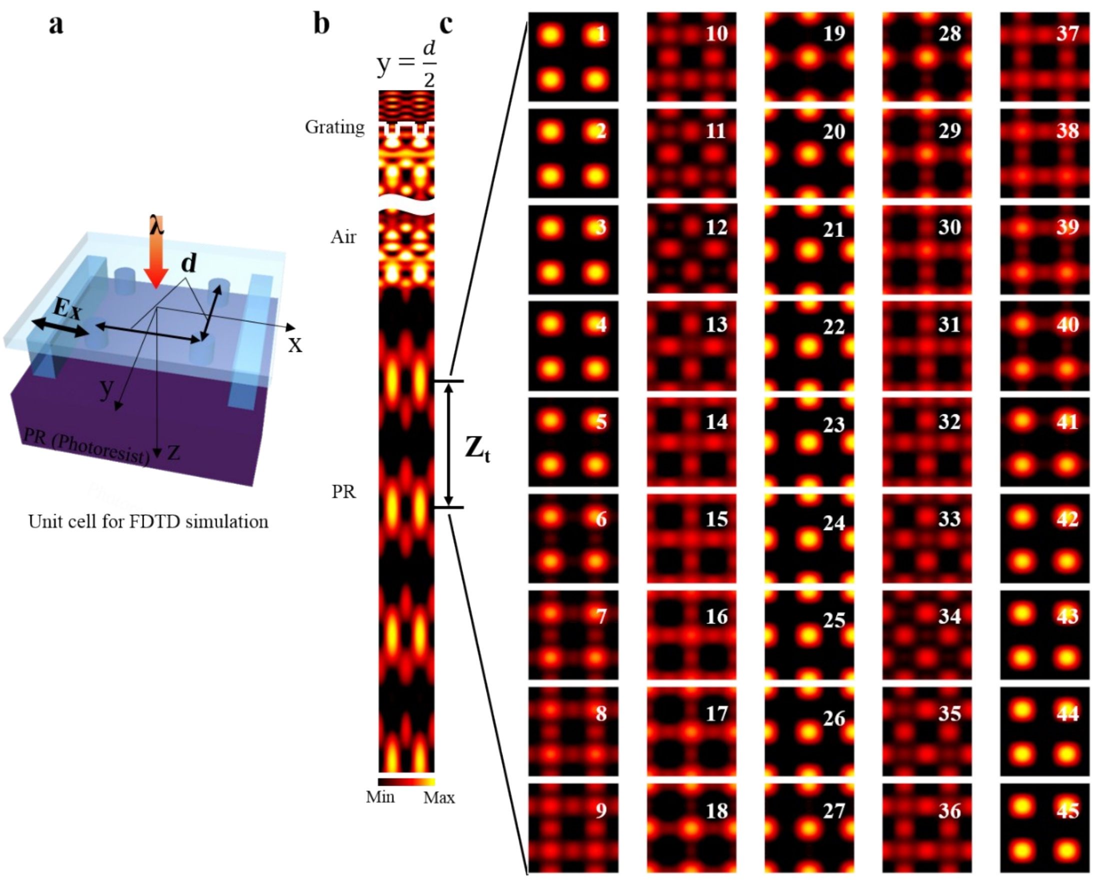

Figure S5. (a) Unit cell of FDTD simulation. (b) Intensity profile at $y = d/2$ plane for $\lambda/d = 0.65$, where Z_t indicates Talbot distance. (c) Horizontal slices of 3D profile in a Talbot distance with equal spacing of $Z_t/44$ along z-direction.

S6. Light propagation patterns from 400 nm and 500 nm diffraction grating with 325 nm light.

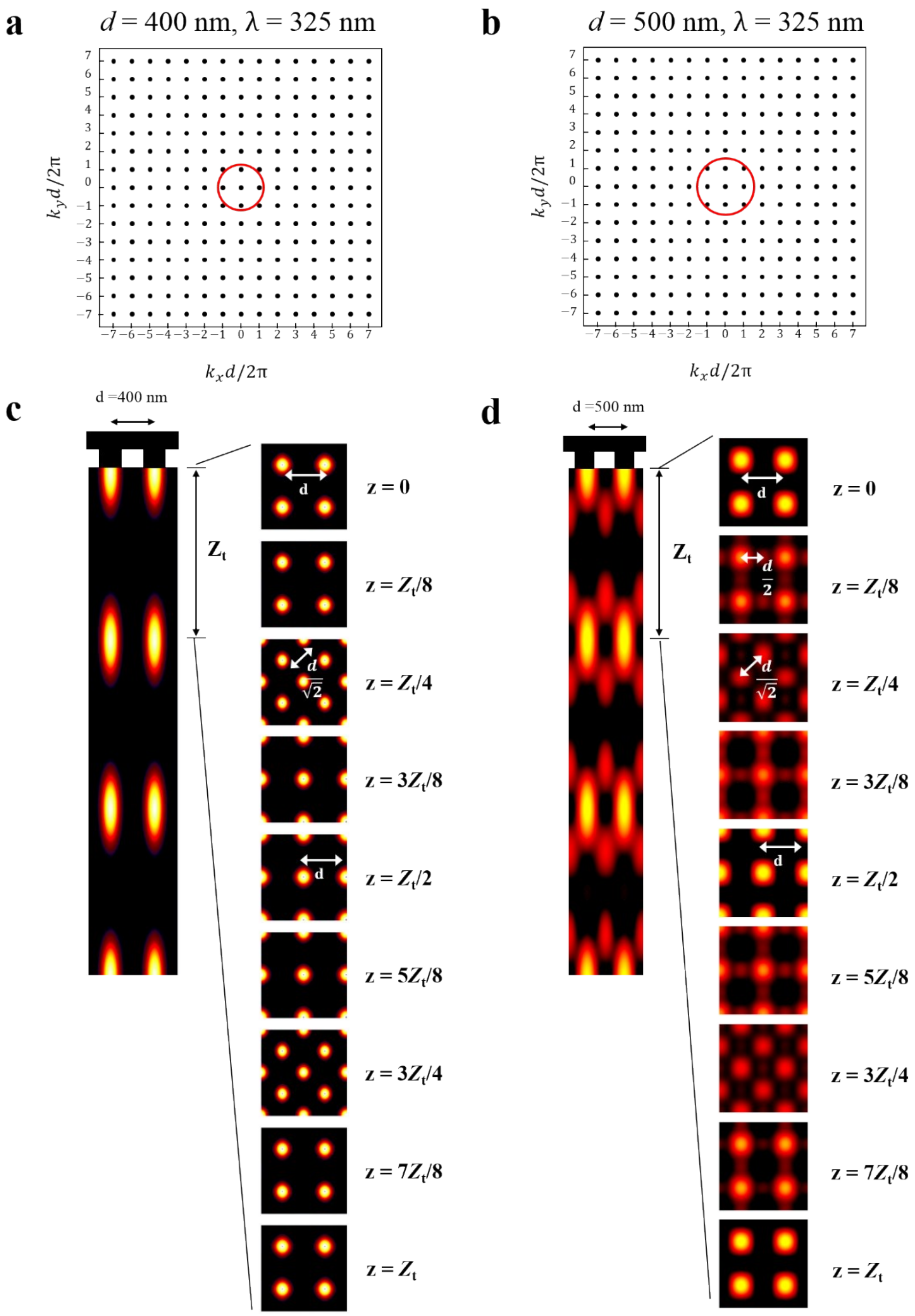

Figure S6. (a, b) Spectrum of *k*-space frequencies for d = 400 nm (a) and d = 500 nm (b), while retaining wavelength is 325 nm. (c, d) Light propagation profile at $y = d/2$ plane and 9 different (x, y) planes calculated by FDTD method, where the Talbot distance, Z_t from different grating period; d = 400 nm (c) and d = 500 nm (d).

S7. Wavelength of m^{th}-order diffraction beam at x- and y-coordinates

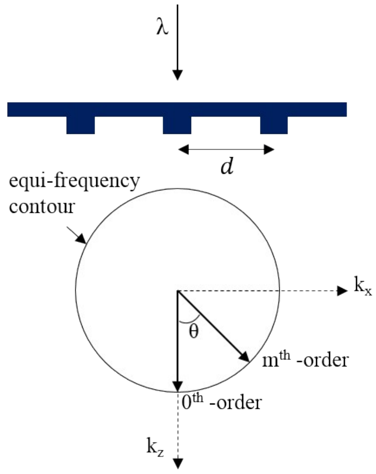

m^{th}-order

$$\text{x-component}: \boldsymbol{\lambda_x} = \frac{2\pi}{|k_x|} = \frac{2\pi\, d}{m\lambda|k|} = \frac{\boldsymbol{d}}{\boldsymbol{m}}$$

$$\left(\sin\theta = \frac{m\lambda}{d} = \frac{|k_x|}{|k|}\right)$$

Figure S7. Wavelength of m^{th}-order diffraction beam at x- and y- coordinates.

S8. Horizontal sections of 3D light intensity profile formed by diffraction beams from 1,500 nm grating from 325 nm light.

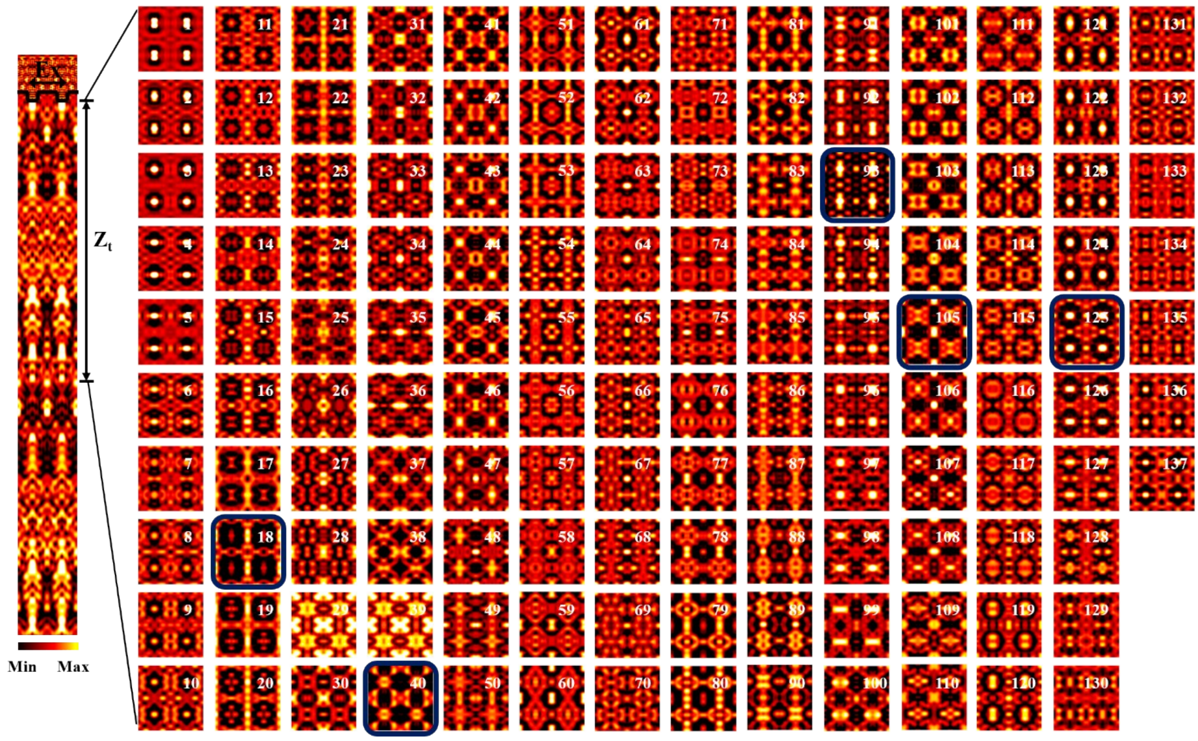

Figure S8. Intensity profile at $y = d/2$ plane for λ/d =0.2167 and horizontal slices of 3D profile in the first Talbot distance with equal spacing of $Z_t/136$ along z-direction. Images of #18, #40, #93, #105 and #125 correspond to SEM images in Figure 3b.

S9. Homogeneity of 2D nanostructures

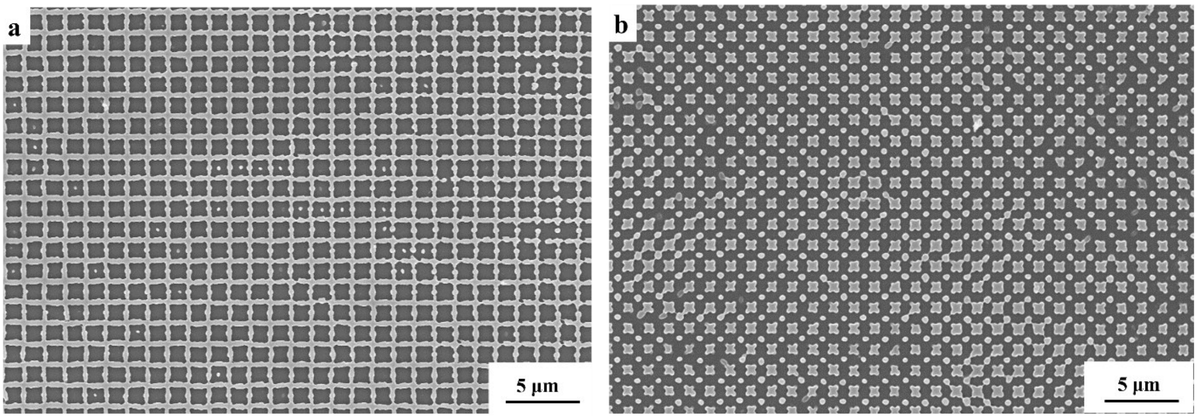

Figure S9. Low magnification image of "1" pattern and "2" pattern of Fig 3b.

S10. Horizontal sections of 3D light intensity profile formed by diffraction beams from 2,000 nm grating from 325 nm light.

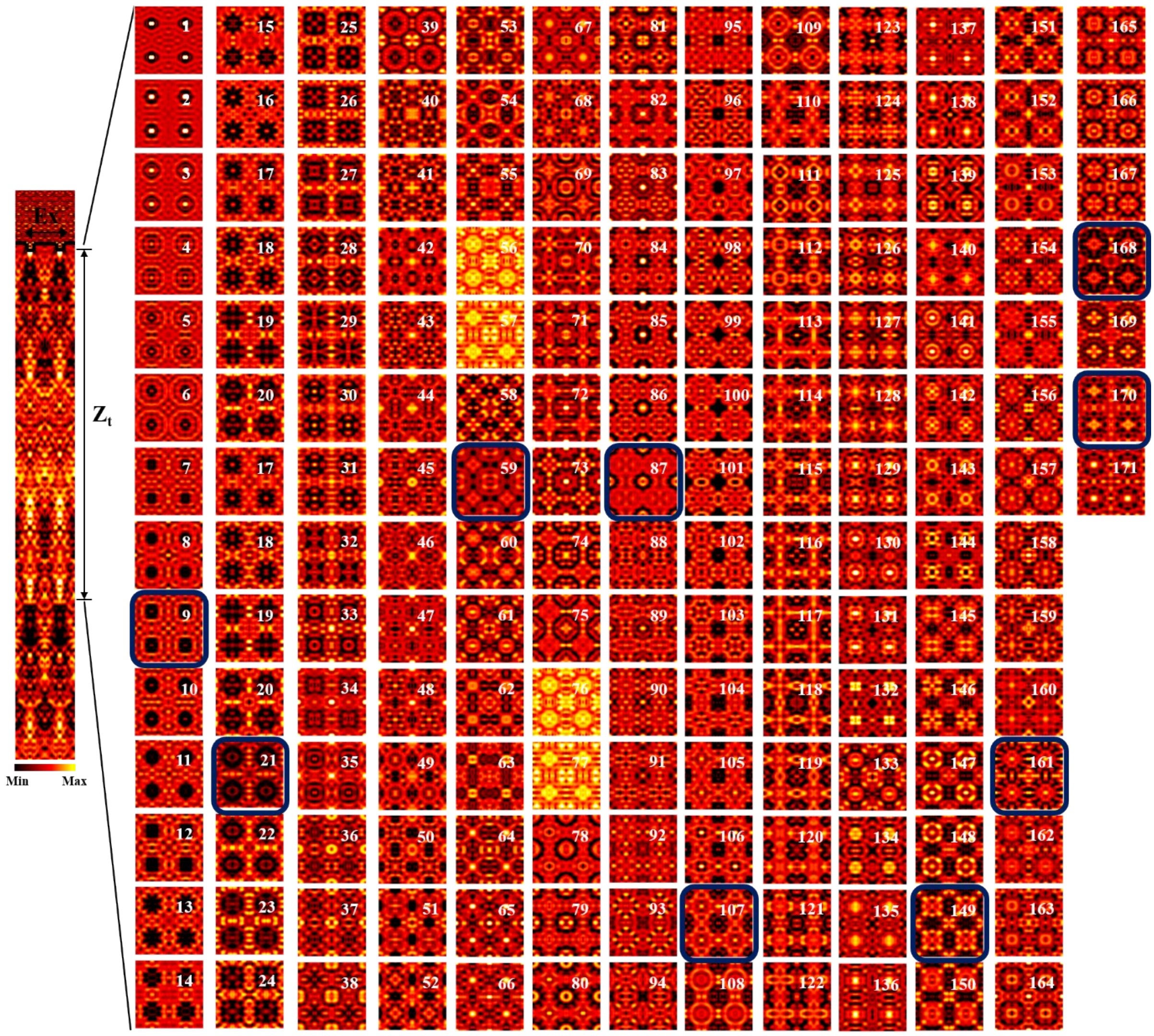

Figure S10. Intensity profile at $y = d/2$ plane for λ/d =0.1625 and horizontal slices of 3D profile in the first Talbot distance with equal spacing of $Z_t/170$ along z-direction. Images of #9, #21, #59, #85, #87, #107, #161, #168 and #170 correspond to SEM images in Figure 4b.

S11. Plasmonic property of reduced size of hierarchical metallic nanostructures

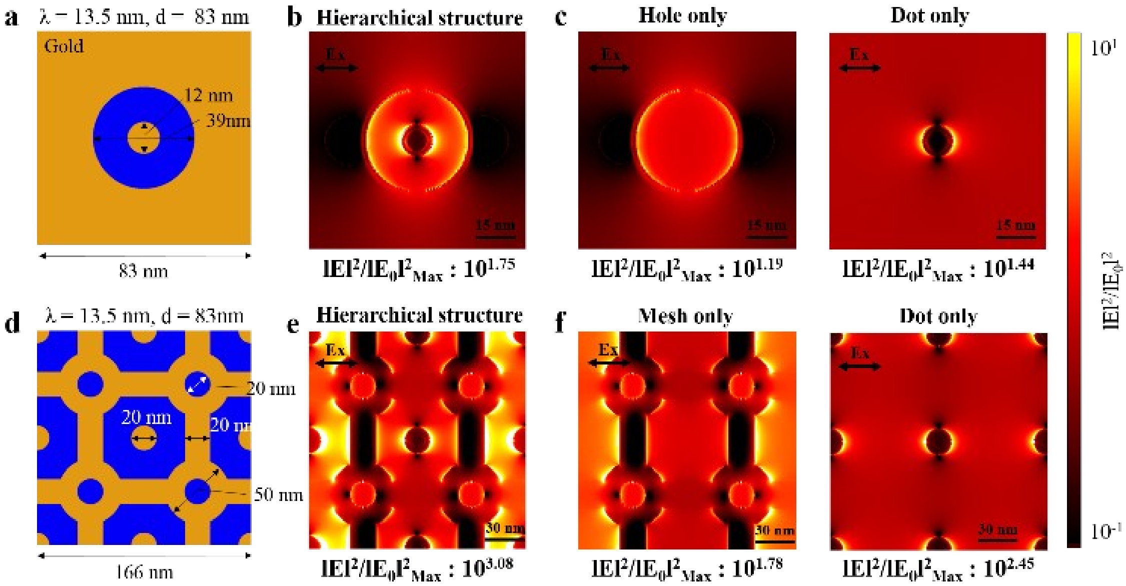

Fig. S11. (a-c) A set of (a) dot-in-hole geometry for FDTD calculation, (b) electric field intensity distribution in the dot-in-hole structure, and (c) intensity distributions in hole structure and dot structure. (d-f) The same set of images for dots-in-mesh geometry.

Hierarchical metal nanostructures with small dimension are appealing for plasmonic applications due to high density of nanogaps. To verify enhancement of light focusing effect for the hierarchical metal nanostructure, we calculate electric field intensity distribution under incident light with wavelength of 633 nm using FDTD method for two different gold nanopatterns with 24-fold reduced size, as shown in Fig. S11. For comparison, two simple nanopatterns, one of which has dots only and the other of which excludes the dots, are employed for each nanopattern. In hierarchical gold nanostructures, the maximum light intensity is observed at the surface of dots as shown in Fig. S11b and e, which are larger than those of simple nanostructures. In details, the maximum intensities, $|E|^2/|E_0|^2_{max}$, from the hierarchical structure of dot-in-hole (Fig. S11b) and single dot (right panel of Fig. S11c) are 56 ($10^{1.75}$) and 27.5 ($10^{1.44}$), respectively; therefore, there are 2-fold enhancement of maximum intensity. The maximum intensities from the hierarchical structure of dots-in-mesh (Fig. S11e) and simple structure of dot array (right panel of Fig. S11f) are 1,200 ($10^{3.08}$) and 282 ($10^{2.45}$), respectively; there are 4-fold enhancement. In addition, the hierarchical structures have wider high intensity regions which is beneficial for sensing application. These enhancement effects are contributed from the complementary interactions between two isolated gold nanostructures. Therefore, hierarchical metal nanostructures with efficient light focusing property are appealing for plasmonic sensors and photovoltaic devices.